Multicomponent Molecular Conductors with Supramolecular Assemblies Prepared from Neutral Iodine-Bearing *p*BIB (*p*-Bis(iodoethynyl)benzene) and Derivatives

Yosuke Kosaka,[1,2,3] **Hiroshi M. Yamamoto,**[2,3] **Akiko Nakao,**[2,3] **and Reizo Kato**[*1,2,3]

[1]Department of Chemistry, Faculty of Science, Saitama University, 255 Shimo-Okubo, Sakura-ku, Saitama 338-8570

[2]RIKEN, 2-1 Hirosawa, Wako 351-0198

[3]JST-CREST, 2-1 Hirosawa, Wako 351-0198

Received October 20, 2005; E-mail: reizo@riken.jp

Organic conductors containing supramolecular assemblies have been obtained from the galvanostatic oxidation of donor molecules with iodine-bearing neutral molecules and halide anions. For the obtained single crystals, X-ray crystal structure analyses along with electrical and magnetic measurements were carried out. $(ET)_3Br(2,5\text{-BIEP})$ (ET = bis-(ethylenedithio)tetrathiafulvalene; 2,5-BIEP = 2,5-bis(iodoethynyl)pyridine) is isostructural with the prototype compound $(ET)_3Br(p\text{BIB})$ (pBIB = p-bis(iodoethynyl)benzene), whereas $(MT)_4X(DFBIB)$ (MT = bis(methylenedithio)-tetrathiafulvalene; DFBIB = 1,4-difluoro-2,5-bis(iodoethynyl)benzene; X = Br and Cl) and $(HMTSF)_4Cl_3(p\text{BIB})_3$-$(PhCl)_x$ (HMTSF = hexamethylenetetraselenafulvalene) differ considerably from $(ET)_3Br(p\text{BIB})$ in structure and, consequently, physical properties. The $(MT)_4X(DFBIB)$ system exhibits a novel two-dimensional donor packing, and represents the first example of the charge ordering in molecular conductors containing supramolecular assemblies based on the halogen bond. $(HMTSF)_4Cl_3(p\text{BIB})_3(PhCl)_x$ is characterized by isolated one-dimensional donor columns.

The construction of crystal frameworks by supramolecular interactions has attracted much attention from the viewpoint of crystal engineering.[1] These non-covalent interactions can generate the crystal architectures, potentially allowing for control of chemical and physical properties. The extensive utility of this technique fascinates not only structural chemists, but also many materials scientists. Introduction of the concept of supramolecular chemistry into the field of molecular conductors is of particular interest, as the conduction properties of molecular conductors are sensitive to crystal structures. The intentional introduction of supramolecular assemblies into molecular conductors can, therefore, be expected to provide a means of designing crystal structures and electrical properties. Our group has been engaged in the development of multicomponent molecular conductors containing halogen···halogen supramolecular interactions. Two isostructural cation radical salts of $(ET)_3X(p\text{BIB})$ (X = Br and Cl) have the organic donor molecule ET with a charge of $+1/3$.[2] This uncommon oxidation state is associated with the supramolecular anionic layer structure. These salts are metallic down to the lowest temperature, and are now recognized to be standard two-dimensional (2D) metals characterized by a very weak electron correlation and simple cylindrical Fermi surface with only one closed orbit. The isostructural compounds $(ET)_3X(DFBIB)$, which can be obtained by replacement of pBIB with the fluorine-substituted neutral molecule DFBIB, also exhibit similar features.[3] A variety of physical measurements of quantum oscillations have been performed for these salts, including angle-dependent magnetoresistance measurement, Shubnikov–de Haars oscillation, and cyclotron resonance analyses.[2,4–7] In $(EDT\text{-}TTF)_4$-

$BrI_2(TIE)_5$ (EDT-TTF = (ethylenedithio)tetrathiafulvalene; TIE = tetraiodoethylene), on the other hand, a one-dimensional (1D) conducting column of donor molecules is surrounded by insulating supramolecular walls composed of TIE molecules and halide anions. Such an architecture can be regarded as a molecular nanowire.[2,8] Conducting salts combining donor and neutral molecules are thus anticipated to yield new compounds that will provide abundant opportunities for the development of functional materials.

However, cation radical salts of donor molecules other than ET have not been studied with pBIB analogues. This paper reports the structural and physical properties of the molecular conductors $(ET)_3Br(2,5\text{-BIEP})$ (**1**), $(MT)_4X(DFBIB)$ (X = Br and Cl; **2a** and **2b**), and $(HMTSF)_4Cl_3(p\text{BIB})_3(PhCl)_x$ (**3**) as new materials.

Experimental

Synthesis. Donor molecules ET, MT,[9] and HMTSF,[10] and neutral molecules pBIB[2] and DFBIB[3] (Fig. 1) were synthesized according to the respective literature procedures. 2,5-BIEP was synthesized from 2,5-dibromopyridine in the same manner as in the literatures.[2,11] Single crystals were grown electrochemically in an H-shaped 20 mL cell under argon and a constant current. (TPP)X (TPP = tetraphenylphosphonium, X = Br and Cl) was employed as the supporting electrolyte and anion source. The detailed conditions of crystal growth are listed in Table 1.

Crystal Structure. Crystal data were collected using an automatic CCD diffractometer (RIGAKU/MSC Mercury) with graphite-monochromated Mo Kα ($\lambda = 0.71070$ Å) radiation at room temperature. Crystal structures were solved by the direct method and refined by the full-matrix least-squares procedure. Non-hydro-
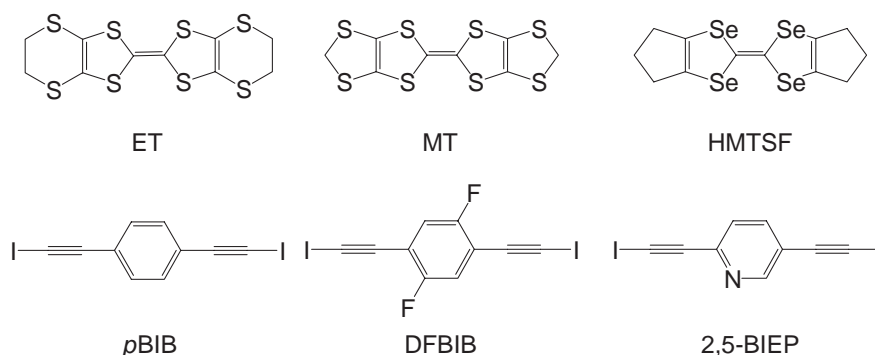
Fig. 1.   Donor molecules (upper) and neutral molecules (lower).

Table 1.   Conditions for Crystal Growth

	1	2a	2b	3
Solvent	CB[a)]:MeOH 95:5	CB:MeOH 95:5	CB:MeOH 95:5	CB:MeOH 95:5
Donor molecules	ET	MT	MT	HMTSF
Neutral molecules	2,5-BIEP	DFBIB	DFBIB	*p*BIB
Supporting electrolyte	TPPBr[b)]	TPPBr	TPPCl	TPPCl
Current/μA	2.5	0.3	0.3	0.5
Temperature/°C	30	20	20	20
Crystal shape	Rectangle	Block	Block	Rectangle

a) CB = chlorobenzene. b) TPP = tetraphenylphosphonium.

Table 2.   Crystallographic Parameters

	$(MT)_4Br(DFBIB)$ 2a	$(MT)_4Cl(DFBIB)$ 2b	$(HMTSF)_4Cl_3(pBIB)_3(PhCl)_x$ 3
Empirical formula	$C_{42}H_{18}BrF_2I_2S_{32}$	$C_{42}H_{18}ClF_2I_2S_{32}$	$C_{78}H_{60}Cl_3I_6Se_{16}$
Formula weight	1920.23	1875.78	3128.48
Crystal system	triclinic	triclinic	monoclinic
Space group	$P\bar{1}$	$P\bar{1}$	$P2_1/n$
$a/\text{Å}$	11.050(4)	11.071(4)	18.229(9)
$b/\text{Å}$	16.372(5)	16.328(5)	18.930(9)
$c/\text{Å}$	8.954(3)	8.895(3)	29.00(1)
$\alpha/\deg$	93.316(4)	93.128(4)	
$\beta/\deg$	104.610(5)	105.176(5)	96.583(3)
$\gamma/\deg$	98.341(4)	97.746(5)	
$V/\text{Å}^3$	1543.2(9)	1530.8(9)	9941(8)
Z	1	1	4
$\rho_{calc}/\text{g cm}^{-3}$	2.066	2.035	2.090
μ/cm^{-1}	2.793	2.205	7.852
Measured reflections	12787	12756	74334
Independent reflections	4522	4442	22244
σ limit	2.0	2.0	4.0
GOF	1.024	1.003	1.780
R,[a)] Rw[b)]	0.0513, 0.1298	0.0564, 0.1504	0.0732, 0.1984

a) $R = \Sigma||F_o| - |F_c||/\Sigma|F_o|$. b) $Rw = [\Sigma w(|F_o| - |F_c|)^2/\Sigma wF_o^2]^{1/2}$.

gen atoms were refined anisotropically, and hydrogen atoms were placed at geometrically calculated positions. For all salts, calculations were performed using the teXsan crystallographic software package from Molecular Structure Co.[12] Application of spherical harmonic absorption correction based on azimuthal scans of several reflections to $(MT)_4Br(DFBIB)$ and $(MT)_4Cl(DFBIB)$ gave transmission factors of 0.6350–0.9256 and 0.6276–0.9369, respectively. Application of numerical absorption correction based on the azimuthal scans of several reflections to $(ET)_3Br(2,5\text{-BIEP})$ and $(HMTSF)_4Cl_3(pBIB)_3(PhCl)_x$ yielded transmission factors

of 0.6883–1.000 and 0.6427–1.000, respectively. Crystallographic data for **2a**, **2b**, and **3** are summarized in Table 2.

Crystallographic data have been deposited with Cambridge Crystallographic Data Centre: Deposition number CCDC-299294 for compound **2a**, CCDC-299295 for compound **2b**, and CCDC-299296 for compound **3**. Copies of the data can be obtained free of charge via http://www.ccdc.cam.ac.uk/conts/retrieving.html (or from the Cambridge Crystallographic Data Centre, 12, Union Road, Cambridge, CB2 1EZ, UK; Fax: +44 1223 336033; e-mail: deposit@ccdc.cam.ac.uk).

Table 3.   Exponents ζ and Ionization Potentials I_p (Ryd.) for the Atomic Orbitals

	S		Se		C		H
	3s	3p	4s	4p	2s	2p	1s
ζ	2.122	1.827	2.44	2.072	1.625	1.625	1.000
$-I_p$ (Ryd.)	1.620	0.770	1.439	0.659	1.573	0.838	1.000

Overlap Integral and Band Calculation.   Overlap integrals (S) between HOMOs of adjacent donor molecules were calculated on the basis of the obtained crystal structures using the extended Hückel MO method and semiempirical parameters (listed in Table 3) for Slater-type atomic orbitals.[13] The sulfur and selenium d atomic orbitals were not included in the calculation. Band structures were obtained by tight-binding band calculations using the transfer integrals (t) with an approximation of $t \approx \varepsilon S$, where ε is a constant corresponding to the order of the energy level of the HOMO (≈ -10 eV).

Electrical Resistivity.   Measurements of the temperature dependence of electrical resistivity were carried out by a standard four-probe dc method. Gold leads (15 µm diameter) were attached to the sample with carbon paste.

Magnetic Susceptibility.   The temperature-dependent magnetic susceptibility of polycrystalline samples (**2a**: 7.6 mg, **2b**: 3.7 mg) was measured using a SQUID magnetometer (Quantum Design MPMS) over a temperature range of 2.0–300 K under an applied magnetic field of 1 T. The diamagnetic contributions of the donors and neutral molecules at room temperature were subtracted from the value observed at room temperature. Pascal's law determined the contribution from anions.[14]

Results and Discussion

Crystal Structures.   (ET)$_3$Br(2,5-BIEP) (1):   Compound **1** is isostructural with (ET)$_3$Br(pBIB).[2] Crystal data: C$_{39}$H$_{27}$BrI$_2$NS$_{24}$, triclinic, space group $P\bar{1}$, $a = 10.20(1)$, $b = 15.51(2)$, $c = 9.33(1)$ Å, $\alpha = 100.46(6)$, $\beta = 106.71(8)$, $\gamma = 77.32(7)°$, $V = 1368(3)$ Å^3, $Z = 1$. Orientational disorder prevented determination of the position of the nitrogen atom on 2,5-BIEP. Despite the poor quality of the crystal, halogen⋯halogen supramolecular assemblies formed by the neutral molecules and Br anions were detected. The I⋯Br distance was found to be ca. 3.2 Å. The Br anions and 2,5-BIEP molecules form 1D supramolecular chains with a period of about 18.5 Å and an inter-chain distance[3] of about 4.92 Å. These features of the supramolecule in **1** are quite similar to those in (ET)$_3$Br(pBIB). No significant differences in donor arrangement were observed between **1** and (ET)$_3$Br(pBIB).

(MT)$_4$X(DFBIB) (X = Br and Cl; 2a and 2b):   Compounds **2a** and **2b** are isostructural. The crystal structures of **2a** are shown in Fig. 2a. The unit cell contains four donor molecules (A, A′, B, and C), two of which (A and A′) are interrelated by the inversion center, with the remaining two (B and C) located on the inversion centers. Both the anion and neutral molecule lie on the inversion centers. The donor molecules exist as a trimer (A–B–A′) and a monomer (C), and are closely packed in a "face-to-edge" mode within the ac plane (Fig. 2b). Molecular conductors having this mode within the donor layer can be found in crystals of so-called κ-type, consisting of the dimers of donor molecules.[15] Similar types, consisting of monomers and dimers[16] or dimers and tetramers,[17]

are further reported, but the present packing motif is different from those in the composite units of donor molecules (monomers and trimers). Therefore, this is a new donor arrangement in molecular conductors.

Supramolecular chains comprising the Br anions and DFBIB molecules extend along the $a + 2c$ direction to form an anionic layer parallel to the ac plane as seen in (ET)$_3$Br-(pBIB) (Fig. 2c). The intermolecular I⋯Br distance (3.25 Å) is considerably shorter than the sum (3.80 Å) of the van der Waals radius of I (1.98 Å) and the anion radius of Br$^-$ (1.82 Å). The 1D chain has a period of approximately 18.5 Å, which is equivalent to the corresponding length in (ET)$_3$Br(pBIB). The benzene ring of the DFBIB molecule in **2a** is situated with a tilt of approximately 18° to the ac plane, while no tilt is observed in (ET)$_3$Br(pBIB). The inter-chain distance thus decreases from 4.92 to 4.84 Å, and the inter-chain angle (defined in Fig. 2c) increases from 47.2 to 69.3°.[3]

The donor:anion ratio in **2a** is 4:1, whereas the ratio is 3:1 in (ET)$_3$Br(pBIB). The difference in the average charge of the donor molecule can be explained by the bulkiness of the donor molecule within the conduction layer. The rigid 2D anionic layer formed by assembly of pBIB–X supramolecules is approximately 90 Å^2 in area and contains one negative charge. The number of donor molecules that the area can accommodate is closely related to the effective area occupied by one donor molecule within the 2D conduction layer.[18] In ET salts with 2D layer structures, one ET molecule is known to occupy about 25–30 Å^2 within the conduction layer. The relatively large area occupied by ET molecules in (ET)$_3$Br(pBIB) is therefore considered reasonable for the unusual 3:1 assembly of the organic metal, resulting in an average charge of $+1/3$. The calculated effective unit area for the MT molecule, on the other hand, is somewhat smaller: 21.1 Å^2 in (MT)$_3$ClO$_4$-(DCE)[19] and 23.1 Å^2 in κ-(MT)$_2$Cu[N(CN)$_2$]Cl.[20] Therefore, four MT molecules can be accommodated in the supramolecular anionic layer of **2a**, which has a unit area of 95.7 Å^2. In this arrangement, the MT molecules have an effective unit area of 23.9 Å^2 ($=95.7/4$).

(HMTSF)$_4$Cl$_3$(pBIB)$_3$(PhCl)$_x$ (3):   The crystal structure of **3** is shown in Fig. 3a. The four donor molecules are crystallographically independent. The unit cell contains two 1D donor columns interrelated by the glide plane, each of which has a repeating unit composed of eight donor molecules. An inversion center is located on the center of each unit (Fig. 3b). The anionic supramolecule in **3** is a quasi-1D chain[8] as shown in Fig. 3c. Three crystallographically independent chains exist in the unit cell, each of which exhibits a period of ca. 18.2 Å and an inter-chain distance of ca. 5 Å. The benzene rings are observed to have two inclinations, $+18$ and $-18°$, from the ac plane. Interstitial spaces, as shown in Fig. 3, are thought to be filled with solvent molecules, chlorobenzene, although no residual peaks were detected by X-ray analysis. The space regarded as a parallelogram (2.1 × 5.7 Å) has dimensions large enough to accommodate chlorobenzenes: length (Cl⋯H), width, and thickness are 8.5, 6.6, and 3.5 Å, respectively,[21] including the van der Waals radii. EPMA (electron probe microanalysis) also supposed the presence of solvent molecules, of which the molecular ratio x can be estimated at ca. 1–1.2. The 1D columns therefore appear to be isolated from each oth-

Y. Kosaka et al.

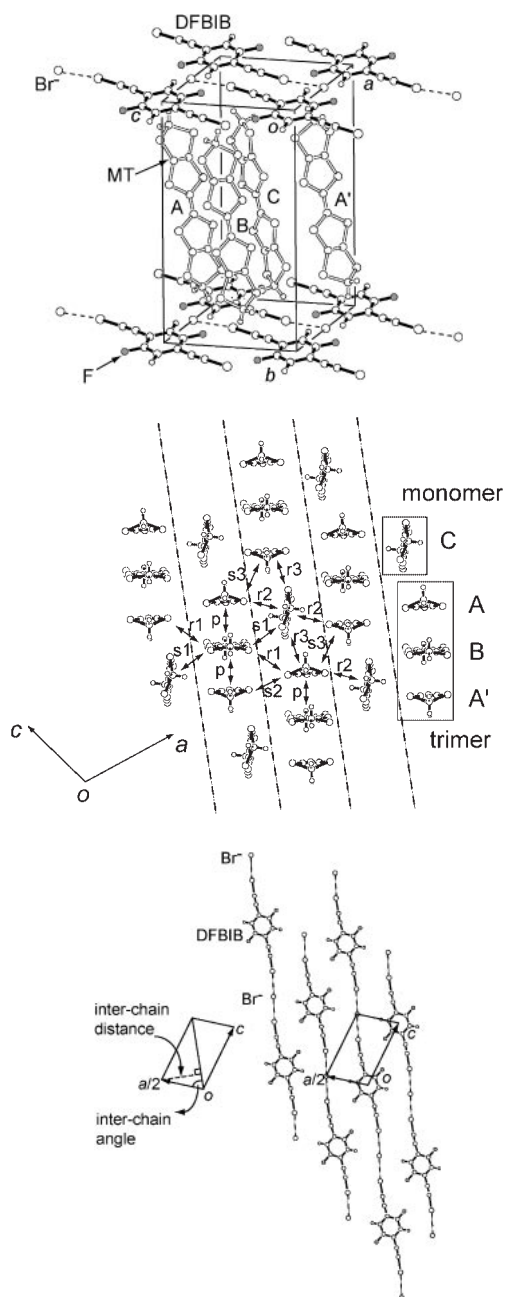Bull. Chem. Soc. Jpn. Vol. 79, No. 7 (2006)   1151

Fig. 2. (a) Crystal packing of **2a**, where dashed lines repre-
sent I⋯Br contacts and F atoms in DFBIB are shaded gray.
(b) Donor arrangement in **2** viewed along the longitudinal
axis of donor molecules, where dashed lines represent
1D chains of DFBIB and the Br anion, and interrelations
between donor molecules are donated alphabetically.
(c) Anionic layer in **2a**, where dashed lines represent I⋯Br
contacts.

Fig. 3. (a) Crystal packing of **3** viewed along the *c* axis,
where dashed lines represent I⋯Cl contacts and dashed cir-
cles donated empty space. (b) Donor arrangement in **3**
viewed along the longitudinal axis of donor molecules.
Overlap integrals (*S*) (overlaps smaller than 1×10^{-3}
are omitted for clarity): $S(\mathbf{c1}) = -25.9$, $S(\mathbf{c2}) = -27.3$,
$S(\mathbf{c3}) = -18.8$, $S(\mathbf{c4}) = -25.6$, and $S(\mathbf{c5}) = -20.6$. (c)
Anionic layer in **3**, where the two inclinations of *p*BIB
are shown in black and white.

er by the supramolecular anionic layer and solvent molecules.
The isolated 1D column structure has also been observed in the
molecular nanowire system $(HMTSF)_2Cl_2(TIE)_3$,[22] in which
case the insulating supramolecules entirely surround the 1D
column. The compound **3** thus represents another type of iso-
lated 1D conducting system.

   Overview.   Except for the minor difference in the benzene
ring inclination, the supramolecular structure of the anionic
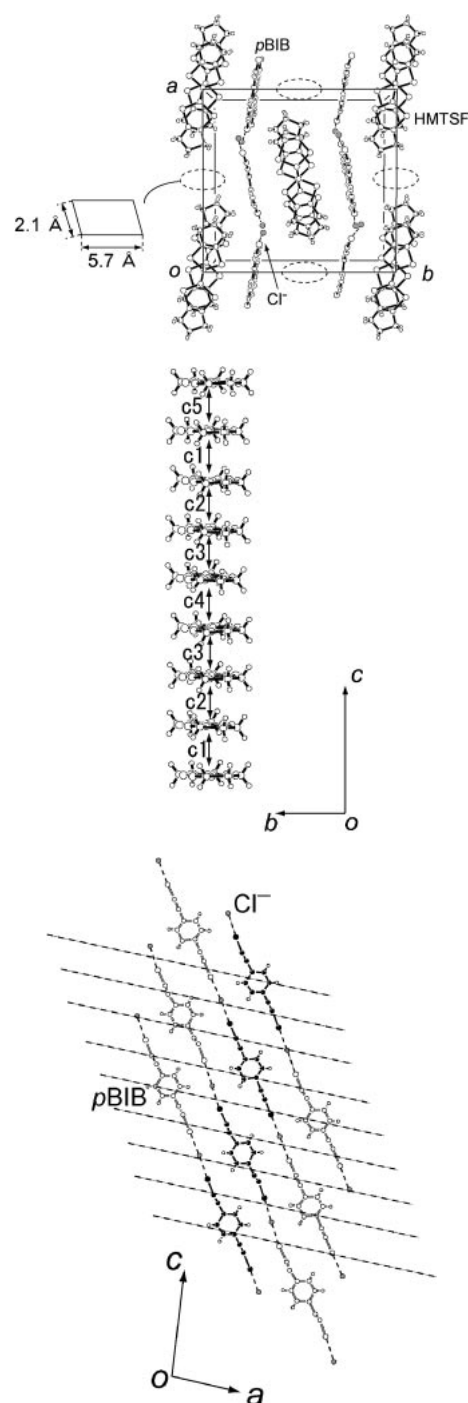
layers for the above four salts and $(ET)_3Br(pBIB)$ are essen-
tially identical. The supramolecular anionic layer can therefore
be considered robust, acting as a host framework that accom-

modates various donor molecules. As we mentioned in a previous paper, the overall crystal structure of such supramolecular conductors is determined by the compatibility of the donor molecule with the supramolecular anionic layer.[8] Subtle changes in the donor molecules, such as replacement of the ethylene group in ET with a methylene group, can have a profound effect on this compatibility, leading to new types of donor packing.

Physical Properties.   (ET)$_3$Br(2,5-BIEP) (1): As shown in Fig. 4, the resistivity of this salt reveals metallic behavior as in the case of (ET)$_3$Br(pBIB). However, the residual resistance ratio for **1** is ca. 10, which is much smaller than that (ca. 10^3) observed for (ET)$_3$Br(pBIB).[3] This difference can be ascribed to the disorder of nitrogen in the neutral molecule 2,5-BIEP.
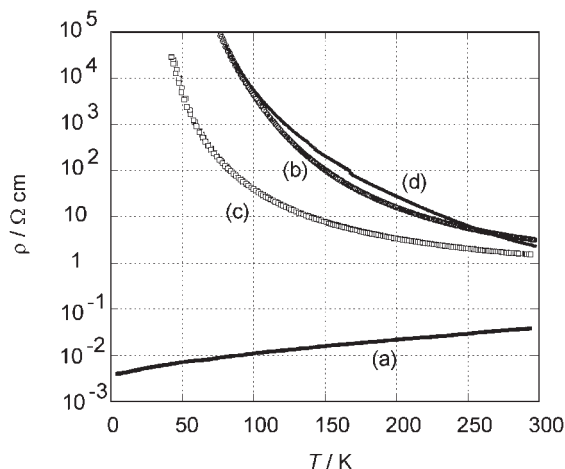

Fig. 4.   Temperature dependence of electrical resistivity for (a) (ET)$_3$Br(2,5-BIEP) (**1**), (b) (MT)$_4$Br(DFBIB) (**2a**), (c) (MT)$_4$Cl(DFBIB) (**2b**), and (d) (HMTSF)$_4$Cl$_3$(pBIB)$_3$-(PhCl)$_x$ (**3**).

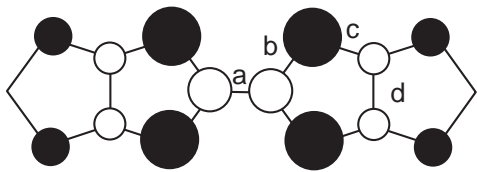Band calculation could not be performed for this salt due to the poor quality of the crystal structure analysis.

(MT)$_4$X(DFBIB) (X = Br and Cl; 2a and 2b): The donor arrangement in **2** is shown in Fig. 2b and the overlap integrals are listed in Table 4. The intermolecular interactions within the trimer (**p**) are stronger than among the other moieties (**r1–r3** and **s1–s3**). Formal charges for the donor molecules in **2** were estimated from the relevant bond lengths (a–d) in the same manner as has been successfully applied to the ET salts.[23] The results have been compared with those of known MT molecules (Table 5). The δ values for both **2a** and **2b** provide the approximate charge of these molecules; that is, molecule B is close to $+0.8$ and the other molecules (A, A′, and C) are close to $+0.1$. The increase or decrease in bond length in the charged molecules is consistent with the symmetry of the HOMO in the MT molecule, which supports the present charge estimation.[28] This charge separation (charge order) of the donor molecules can be inferred from these results. More accurate charge values for **2** could not be determined due to the limited number of bond lengths obtained for the MT molecules. Most notably, the positive charge concentrates on molecule B, which is surrounded by other near-neutral molecules. The positively charged molecules are thus isolated from each other, resulting in reduction of the nearest-neighbor Coulomb repulsion.

Figure 5 shows the variation in the magnetic susceptibility (χ) for **2a** and **2b** with temperature. Both values increase from 300 to 80 K, below which the anti-ferromagnetic interaction

Table 4.   The Overlap Integrals (S) among HOMOs ($\times 10^{-3}$) for **2**

	r1	r2	r3	s1	s2	s3	p
2a	−2.13	−2.42	−2.16	−5.26	1.43	−3.89	−11.6
2b	−2.15	−2.37	−2.30	−5.00	1.38	−4.43	−11.9

Table 5.   List of the Bond Lengths (Å), Formal Charges, and the δ Values (Å) for MT Salts[a]

		Charge	a	b	c	d	δ
MT (neutral)[24]		0	1.327	1.767(3)	1.738(1)	1.334(0)	0.844
(MT)SbF$_6$[25]		1	1.361	1.729(2)	1.724(1)	1.347(0)	0.745
(MT)[Ag(CN)$_2$][26]		1	1.407	1.728(0)	1.723(0)	1.353(0)	0.691
(MT)I$_3$[27]		1	1.381	1.732(5)	1.725(3)	1.357(2)	0.719
Averaged length			1.383(19)	1.730(2)	1.724(1)	1.352(4)	0.719(22)
2a	A (A′)	—	1.339	1.764(8)	1.739(4)	1.341(4)	0.823
	B	—	1.384	1.740(4)	1.734(1)	1.348(0)	0.742
	C	—	1.343	1.765(11)	1.744(0)	1.341(0)	0.825
2b	A (A′)	—	1.353	1.761(5)	1.734(3)	1.347(7)	0.795
	B	—	1.382	1.742(1)	1.741(3)	1.352(0)	0.749
	C	—	1.353	1.760(12)	1.748(3)	1.332(0)	0.823

a) Molecule A (A′), B, and C are in **2**. Parenthesized values are the statistical standard deviation ($\times 10^{-3}$) in each bond length. δ values given by $(b + c) - (a + d)$ are the same manner as in Ref. 23.
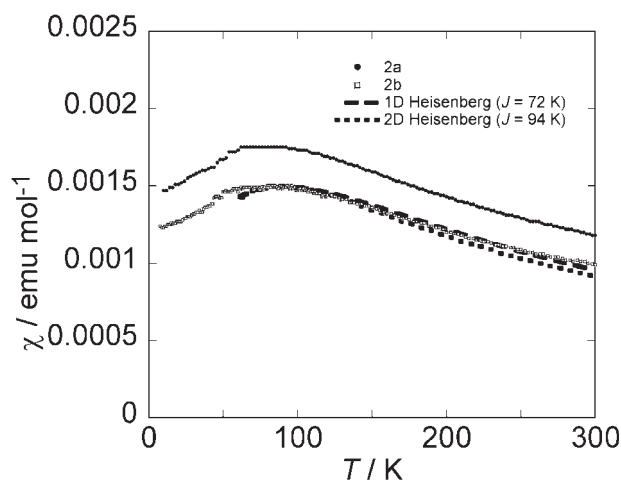
Fig. 5. Variation in magnetic susceptibility of **2a** and **2b** with temperature.

between local moments becomes dominant. Because the behaviors of χ values are very similar in their peak temperatures and gradients, the difference in the absolute value between **2a** and **2b** may be attributed to an experimental error caused by the correction values of diamagnetic contributions. The behaviors resemble that of the 2D square lattice Heisenberg model (The Hamiltonian are described as $H = J \sum_{\langle i,j \rangle} \vec{S}_i \cdot \vec{S}_j$) with $J = 72\,\mathrm{K}$[29] or the 1D linear chain Heisenberg model (The Hamiltonian are described as $H = 2J \sum_i \vec{S}_{2t} \cdot \vec{S}_{2i-1} + \vec{S}_{2t} \cdot \vec{S}_{2i+1}$) with $J = 94\,\mathrm{K}$.[30] Both of the calculated peak temperatures (87 K) are different from those for **2a** and **2b**, suggesting the deviation of the system from an ideal 1D or 2D model. The main reason for the discrepancies should be the partial distribution of the charges and spins ($+0.8$ for molecule B and $+0.1$ for the others) that prevent us from estimating effective interactions between local moments. The lack of appropriate theoretical calculations is also an obstacle in examining precise behavior. Regardless, these results suggest the presence of local spins, and thus, **2a** and **2b** are not band insulators, which is consistent with our assumption that the compounds are in the charge-ordering state.

The electrical resistivity measurement exhibits that **2a** and **2b** are semiconductors with activation energies of 90 and 40 meV, respectively (Fig. 4).

The isolation of positively charged molecules represents the first example of charge separation in the series of multicomponent molecular conductors based on a halogen bond. Charge separation (or charge order) is observed in many molecular conductors including θ-$(ET)_2RbZn(SCN)_4$,[31] $(EDO\text{-}TTF)_2$-PF_6 $(EDO\text{-}TTF = (ethylenedioxy)tetrathiafulvalene)$,[32] and α-$(ET)_2I_3$,[33] and remains a subject of intense research owing to the crucial role of this phenomenon in determining the electronic properties and functionally of these materials. It has recently been reported that the charge-ordering state is destroyed by photo irradiation, which induces an insulator–metal transition in $(EDO\text{-}TTF)_2PF_6$[34] and α-$(ET)_2I_3$.[35] Our present materials can be candidates with such a phenomenon.

$(HMTSF)_4Cl_3(pBIB)_3(PhCl)_x$ (3): Figure 3b shows the overlap integrals in **3**. The compound exhibits 1D character. Although two 1D donor columns exist in the unit cell, the interaction between columns is negligible. No appreciable difference was observed among the bond lengths of the four crystallographically independent donor molecules, indicating that all donor molecules have similar charges. The repeating unit of the 1D column is composed of eight donor molecules. The 1D energy band is thus divided into eight branches. The band filling is $+5/8$ due to a 4:3 donor:anion ratio, and thus, **3** is a band insulator with a relatively narrow band gap estimated to be ca. 60 meV. As shown in Fig. 4, the temperature dependence of electrical resistivity reveals semiconductive behavior with an activation energy of ca. 80 meV, which is in reasonable agreement with the result of band calculations.

Conclusion

Four multi-component molecular conductors with supramolecular interactions containing *p*BIB analogues were characterized with respect to structure and physical properties. The rigid anionic layer formed by the *p*BIB analogue and halide anion accommodates various donor molecules. $(ET)_3Br$-$(2,5\text{-}BIEP)$ (**1**) is isostructural with the prototype compound $(ET)_3Br(pBIB)$, and is metallic down to the lowest temperature examined. $(MT)_4Br(DFBIB)$ (**2a**) and $(MT)_4Cl(DFBIB)$ (**2b**) exhibit a new type of donor arrangement based on a face-to-edge packing of the trimer and the monomer. Magnetic susceptibility measurement reveals the existence of localized spins, resulting from the charge-ordering state confirmed by the bond lengths analysis of the donor molecules. The electrical resistivity shows semiconductive behavior due to the charge-ordering state. This is the first example of the charge-ordering state in a series of multicomponent molecular conductors based on a halogen bond. $(HMTSF)_4Cl_3(pBIB)_3(PhCl)_x$ (**3**) consists of rigid 1D donor columns that are isolated from each other by the supramolecular anionic layer and solvent molecules. The compound **3** is a semiconductor with low activation energy, consistent with the result of the tight-binding band calculations. These results demonstrate the ability of *p*BIB-based supramolecular assemblies to combine various donor molecules and produce unique packing motifs.

References

1 G. R. Desiraju, *Angew. Chem., Int. Ed. Engl.* **1995**, *34*, 2311.

2 H. M. Yamamoto, J.-I. Yamaura, R. Kato, *J. Am. Chem. Soc.* **1998**, *120*, 5905.

3 H. M. Yamamoto, R. Maeda, J.-I. Yamaura, R. Kato, *J. Mater. Chem.* **2001**, *11*, 1034.

4 S. Yasuzuka, C. Terakura, T. Terashima, T. Yakabe, Y. Terai, H. M. Yamamoto, J.-I. Yamaura, R. Maeda, R. Kato, S. Uji, *Synth. Met.* **2003**, *133–134*, 169.

5 S. Yasuzuka, S. Uji, H. M. Yamamoto, J.-I. Yamaura, C. Terakura, T. Terashima, T. Yakabe, Y. Terai, R. Maeda, R. Kato,

1154   *Bull. Chem. Soc. Jpn. Vol. 79, No. 7 (2006)*

Multicomponent Supramolecular Conductor

J. Phys. Soc. Jpn. **2005**, *74*, 679.

6   Y. Oshima, H. Ohta, K. Koyama, M. Motokawa, H. M. Yamamoto, R. Kato, M. Tamura, Y. Nishio, K. Kajita, *J. Phys. Soc. Jpn.* **2003**, *72*, 143.

7   R. Jindo, S. Sugawara, N. Tajima, H. M. Yamamoto, R. Kato, Y. Nishio, K. Kajita, *J. Phys. Soc. Jpn.* **2006**, *75*, 013705.

8   H. M. Yamamoto, *RIKEN Rev.* **2002**, *46*, 3.

9   M. Mizuno, A. F. Garito, M. Cava, *J. Chem. Soc., Chem. Commun.* **1978**, 18; R. Kato, T. Mori, A. Kobayashi, Y. Sasaki, H. Kobayashi, *Chem. Lett.* **1984**, 781.

10   K. Bechgaard, D. O. Cowan, A. N. Bloch, *Mol. Cryst. Liq. Cryst.* **1976**, *32*, 227; R. D. McCullough, D. O. Cowan, *J. Org. Chem.* **1985**, *50*, 4646.

11   S. Takahashi, Y. Kuroyama, K. Sonogashira, N. Hagihara, *Synthesis* **1980**, 627.

12   *teXsan: Crystal Structure Analysis Package*, Molecular Structure Co., The Woodlands, TX, **1985** and **1999**.

13   E. Canadell, I. E.-I. Rachidi, S. Ravy, J. P. Pouget, L. Brossard, J. P. Legros, *J. Phys. Fr.* **1989**, *50*, 2967.

14   *Kagaku Binran, Kisohen II*, Maruzen, Tokyo, **1989**, Ver. 3, p. II-508.

15   T. Mori, H. Mori, S. Tanaka, *Bull. Chem. Soc. Jpn.* **1999**, *72*, 179.

16   N. D. Kushch, O. N. Kazheva, V. V. Gritsenko, L. I. Buravov, K. V. Van, O. A. Dyachenko, *Synth. Met.* **2001**, *123*, 171.

17   K. Takimiya, Y. Kataoka, Y. Nakamura, Y. Aso, T. Otsubo, *Synthesis* **2004**, 1315.

18   H. M. Yamamoto, R. Kato, *Chem. Lett.* **2000**, 970.

19   R. Kato, H. Kobayashi, A. Kobayashi, Y. Sasaki, *Chem. Lett.* **1984**, 1693.

20   T. Naito, K. Bun, A. Miyamoto, H. Kobayashi, H. Sawa, R. Kato, A. Kobayashi, *Synth. Met.* **1993**, *55–57*, 2234.

21   D. Andre, R. Fourme, M. Renaud, *Acta Crystallogr., Sect. B* **1971**, *27*, 2371.

22   H. M. Yamamoto, R. Maeda, J.-I. Yamaura, R. Kato, *Synth. Met.* **2001**, *120*, 781.

23   P. Guionneau, C. J. Kepert, D. Chasseau, M. R. Truter, P. Day, *Synth. Met.* **1997**, *86*, 479.

24   R. Kato, H. Kobayashi, A. Kobayashi, Y. Sasaki, *Chem. Lett.* **1985**, 1231.

25   P. J. Nigrey, E. Duesler, H. H. Wang, J. M. Williams, *Acta Crystallogr., Sect. C* **1987**, *43*, 1073.

26   B. Morosin, P. J. Nigrey, *Acta Crystallogr., Sect. C* **1992**, *48*, 1216.

27   T. Sugano, S. Sato, M. Konno, M. Kinoshita, *Acta Crystallogr., Sect. C* **1988**, *44*, 1764.

28   R. Kato, H. Kobayashi, T. Mori, A. Kobayashi, Y. Sasaki, *Solid State Commun.* **1985**, *55*, 387.

29   F. M. Woodward, A. S. Albrecht, C. M. Wynn, C. P. Landee, M. M. Turnbull, *Phys. Rev. B* **2002**, *65*, 144412.

30   J. W. Hall, W. E. Marsh, R. R. Weller, W. E. Hatfield, *Inorg. Chem.* **1981**, *20*, 1033.

31   R. Chiba, H. M. Yamamoto, K. Hiraki, T. Nakamura, T. Takahashi, *Synth. Met.* **2001**, *120*, 919.

32   S. Aoyagi, K. Kato, A. Ota, H. Yamochi, G. Saito, H. Suematsu, M. Sakata, M. Tanaka, *Angew. Chem., Int. Ed.* **2004**, *43*, 3670.

33   Y. Takano, K. Hiraki, H. M. Yamamoto, T. Nakamura, T. Takahashi, *J. Phys. Chem. Solids* **2001**, *62*, 393.

34   M. Chollet, L. Guerin, N. Uchida, S. Fukaya, H. Shimoda, T. Ishikawa, K. Matsuda, T. Hasegawa, A. Ota, H. Yamochi, G. Saito, R. Tazaki, S. Adachi, S. Koshihara, *Science* **2005**, *307*, 86.

35   N. Tajima, J. Fujisawa, N. Naka, T. Ishihara, R. Kato, Y. Nishio, K. Kajita, *J. Phys. Soc. Jpn.* **2005**, *74*, 511.